

Modelling and simulating Lenski’s long-term evolution experiment

Ellen Baake Adrián González Casanova
Sebastian Probst Anton Wakolbinger

January 12, 2019

Abstract

We revisit the model by Wisser, Ribeck, and Lenski (Science **342** (2013), 1364–1367), which describes how the mean fitness increases over time due to beneficial mutations in Lenski’s long-term evolution experiment. We develop the model further both conceptually and mathematically. Conceptually, we describe the experiment with the help of a Cannings model with mutation and selection, where the latter includes diminishing returns epistasis. The analysis sheds light on the growth dynamics within every single day and reveals a runtime effect, that is, the shortening of the daily growth period with increasing fitness; and it allows to clarify the contribution of epistasis to the mean fitness curve. Mathematically, we present rigorous results in terms of a law of large numbers (in the limit of infinite population size and for a certain asymptotic parameter regime), as well as approximations based on heuristics and supported by simulations for finite populations.

1 Introduction

One of the most famous instances in experimental evolution is Lenski’s long-term evolution experiment or LTEE (Lenski et al. 1991; Wisser et al. 2013; Tenaillon et al. 2016; Good et al. 2017). Over a period of 30 years, populations of *Escherichia coli* maintained by daily serial transfer have accumulated mutations, resulting in a steady increase in fitness. The mean fitness is observed to be a concave function of time, that is, fitness increases more slowly as time goes by. Wisser et al. (2013) formulated a first theoretical model that builds on the underlying processes, namely mutation, selection, and genetic drift, and obtained a good agreement with the data. The model invites further development, both mathematically and conceptually; this is the motivation for this paper.

Let us briefly describe the LTEE, the model by Wisser et al. (2013), and the goal and outline of this paper.

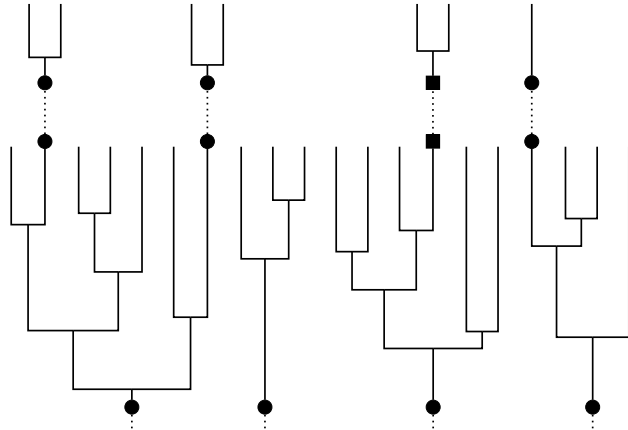


Figure 1: Illustration of some day $i - 1$ (and the beginning of day i) of Lenski's LTEE with 4 founder individuals (bullets), their offspring trees within day $i - 1$, and the sampling from day $i - 1$ to i (dotted), for an average clone size of 5. The second founder from the left at day $i - 1$ (and its offspring) is lost due to the sampling, and the second founder from the right at day i carries a new beneficial mutation (indicated by the square).

Lenski's LTEE. Every morning, Lenski's LTEE starts with a sample of $\approx 5 \cdot 10^6$ *Escherichia coli* bacteria in a defined amount of fresh minimal glucose medium. During the day (possibly after a lag phase), the bacteria divide until the nutrients are used up; this is the case when the population has reached ≈ 100 times its original size. The cells then stop dividing and enter a starvation phase. At the end of the growth period, there are therefore $\approx 5 \cdot 10^8$ bacteria, namely, $\approx 5 \cdot 10^6$ clones each of average size ≈ 100 , see Fig. 1. At the next morning, one takes a random sample of $\approx 5 \cdot 10^6$ out of the $\approx 5 \cdot 10^8$ cells, puts them into fresh medium, and the game is repeated; the sampled individuals are the roots of the new offspring trees. Note that the number of offspring an individual contributes to the next generation is random; it is 1 on average, but can also be 0 or greater than one.

Lenski started 12 replicates of the experiment in 1988, and since then it has been running without interruption. The goal of the experiment is to observe evolution in real time. Indeed, the bacteria evolve via beneficial mutations, which allow them to adapt to the environment by, for example, using the nutrients more efficiently, and thus to reproduce faster. Of course neutral and deleterious mutations are more frequent than beneficial ones (Eyre-Walker and Keightley 2007), but neutral and slightly deleterious mutations will, by definition, contribute nothing or little to the adaptive process, even if they go to fixation; and strongly deleterious ones get lost quickly.

One special feature of the LTEE is that samples are frozen at regular inter-

vals. They can be brought back to life at any time for the purpose of comparison and thus form a living fossil record. In particular, one can, at any day i , compare the current population with the initial (day 0) population via the following *competition experiment* (Lenski and Travisano 1994; Wisler et al. 2013). A sample from the day-0 population and one from the day- i population, each of size $\approx 2.5 \cdot 10^6$ cells, are grown together until the nutrients are used up (say this is the case at time T_i). One then defines

$$\text{empirical relative fitness at day } i = \frac{\log(Y_i(T_i)/Y_i(0))}{\log(Y_0(T_i)/Y_0(0))}, \quad (1)$$

where, for $T = 0$ and $T = T_i$, $Y_i(T)$ and $Y_0(T)$ are the sizes at time T of the populations grown from the day- i sample and the day-0 sample, respectively. Note that the empirical relative fitness is a random quantity, whose outcome will vary from replicate to replicate. Fig. 2 shows the time course of the empirical relative fitness averaged over the replicate populations, over 21 years as observed by Wisler et al. (2013). Obviously, the mean fitness has a tendency to increase, but the increase levels off, which leads to a conspicuous concave shape.

The WRL model and its building blocks. In the same 2013 paper, Wisler, Ribbeck, and Lenski presented their model to explain the shape of the fitness curve. This model, henceforth referred to as WRL, takes into account two important effects, namely, (*diminishing returns*) *epistasis* and *clonal interference*. Diminishing returns epistasis (see, e.g., Bürger (2000, p. 74) or Phillips et al. (2000)) means that the beneficial effect of mutations decreases with increasing fitness. Clonal interference (Gerrish and Lenski 1998; Gerrish 2001; Park and Krug 2007) refers to the situation of two (or more) beneficial mutations present in the population at the same time. They then compete with each other and, in the end, only one of them will be established in the population; an effect that slows down adaption (when measured against the stream of incoming mutations). Both epistasis and clonal interference may be considered as interactions of mutations (within one individual in the case of epistasis, between different individuals in the case of clonal interference).

The arguments of Wisler et al. (2013) lead to the following power law for the relative fitness \tilde{f} :

$$\tilde{f}(k) = (1 + \beta k)^{\frac{1}{2g}} \quad (2)$$

with parameters $\beta > 0$ and $g > 0$. Here g is some measure of the strength of epistasis, and β is a time-scaling constant, which also takes into account the effect of clonal interference. Furthermore, k is time with one generation (which is here the mean doubling time) as unit, so

$$i = \left\lfloor \frac{k}{\log_2 100} \right\rfloor \approx \frac{k}{6.6}. \quad (3)$$

The red solid line in Fig. 2 shows the best fit of this curve to the data of all 12 replicate populations, as obtained by Wisler et al. (2013), with parameter

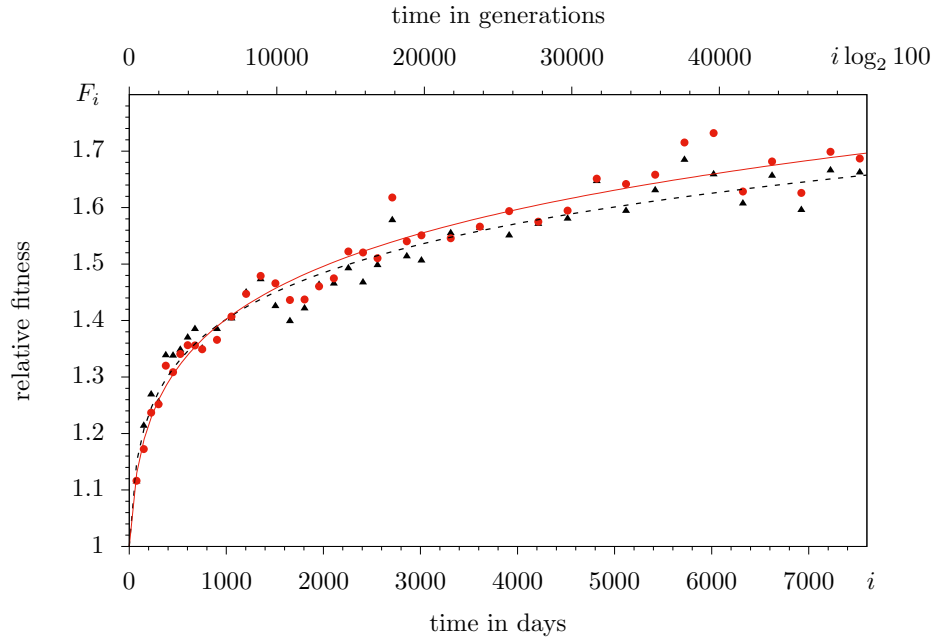


Figure 2: Empirical relative fitness averaged over all 12 populations (red bullets) and averaged over the 6 populations (black triangles) that kept the original (low) mutation probability (that is, hypermutator strains were excluded); corresponding power laws (2) with $\hat{g} = 5.3$, $\hat{\beta} = 5.1 \cdot 10^{-3}$ (red solid line) and $\hat{g} = 6.0$, $\hat{\beta} = 8.7 \cdot 10^{-3}$ (black dashed line), respectively. Data and parameters according to Fig. 2A and Table S4 of Wisler et al. (2013). Our parameters obtained via `NonlinearModelFit` of `Wolfram Mathematica 11` only differ in the third digits.

estimates $\hat{g} = 5.3$ and $\hat{\beta} = 5.2 \cdot 10^{-3}$ (here and in what follows, parameter values estimated from the data are indicated by a hat, and numbers are rounded to 2 digits); the black dashed curve is the corresponding fit after exclusion of those populations that evolved into hypermutator strains. In line with (1) and (3), we take *days* as our discrete time units, rather than doubling times (this will pay off in Secs. 2 and 3); so $\log_2 100 \approx 6.6$ generations in Fig. 2 correspond to one day, and the total of 50000 generations correspond to around 7525 days. We refrain from recapitulating the details of the WRL model at this point, but refer the reader to the original article, and will also come back to this in Sec. 4.

Goal and outline of this paper. Our goal in this paper is to elaborate on the WRL model and its foundations in various respects. First, we will recall in Sec. 2 that the design of the LTEE provides an example of what is known in population genetics as a *Cannings model* (Ewens 2004, Ch. 3.3), which is naturally extended to a situation incorporating selection here. As noted by González Casanova et al. (2016), this is due to the daily sampling and the resulting (approximately) constant population size at the beginning of each day.

Second, in addition to the contributions of epistasis and clonal interference, we will also clarify the role of the *design of the experiment* to the shape of the fitness curve. While epistasis and clonal interference are already inherent in the WRL model, the design of the experiment, namely the daily cycles and the sampling scheme, have not explicitly been taken into account so far, and will turn out to play a clarifying role. Third, we aim at a rigorous mathematical treatment where possible; in particular, we will review a law of large numbers (that is a deterministic limit) in a suitable parameter regime as $N \rightarrow \infty$. The latter was proved by González Casanova et al. (2016) and published in a mathematical journal. In Sec. 2, we will recapitulate their model (referred to as GKWY) and explain the results for a biological readership. Fourth, we will consider the resulting stochastic effects in a system whose parameters are obtained from a fit to data observed in the LTEE (and which thus naturally differs from its infinite population limit). This will be done at the end of Sec. 2 for the GKWY model, and in Sec. 3 for a model including clonal interference, with different heuristics for the case of deterministic and random fitness increments. Here we do not prove a law of large numbers, but obtain approximations with the help of moment closure. In Sec. 4, we will thoroughly discuss various modelling aspects, in particular the notion of epistasis, in the context of both the WRL and the GKWY models; this will also clarify the meaning of the parameters g and β in (2).

2 A probabilistic model for the LTEE and its law of large numbers

The GKWY model takes into account two different dynamics, namely, the dynamics *within each individual day*, and the dynamics *from day to day*, together

with a suitable *scaling regime*. The resulting *relative fitness process* is proved to converge, in the $N \rightarrow \infty$ limit, to a power law equivalent to (2); that is, the power law arises as a *law of large numbers*. We explain this here with the help of an appropriate *heuristics*. In what follows, we present these building blocks and perform a first *reality check*.

Intraday dynamics. Let T be (continuous) physical time within a day, with $T = 0$ corresponding to the beginning of the growth phase (that is, we discount the lag phase). Day i starts with N founder individuals ($N \approx 5 \cdot 10^6$ in the experiment). The reproduction rate (or *Malthusian fitness*) of founder individual j at day i is R_{ij} , $i \geq 0, 1 \leq j \leq N$. It is assumed that at day 0 all individuals have identical rates, $R_{0j} \equiv R_0$, so the population is *homogeneous*. Offspring inherit the reproduction rates from their parents.

We use dimensionless variables right away. Therefore we denote by

$$t = R_0 T \quad \text{and} \quad (4)$$

$$r_{ij} = \frac{R_{ij}}{R_0} \quad (5)$$

dimensionless time and rates, so that on the time scale t there is, on average, one split per time unit at the beginning of the experiment (this unit is 55 minutes, cf. Barrick et al. (2009)) and $r_{0j} \equiv 1$. In this paragraph, we consider the r_{ij} as given (non-random) numbers.

There are then N independent *Yule processes* at day i ; all descendants of founder individual j (the members of the j -clone) branch at rate r_{ij} , independently of each other. They do so until $t = \sigma_i$, where σ_i is the duration of the growth phase on day i . We define σ_i as the value of t that satisfies

$$\mathbb{E}(\text{population size at time } t) = \sum_{j=1}^N e^{r_{ij}t} = \gamma N, \quad (6)$$

where γ is the multiplication factor of the population within a day. Equivalently, γ is the average clone size, or the dilution factor from day to day ($\gamma \approx 100$ in the experiment). Note that the Yule processes are stochastic, so the population size at time t is, in fact, random; in the definition of σ_i , we have idealised by replacing this random quantity by its expectation. Since N is very large, this is well justified, because the fluctuations of the random time needed to grow to a factor 100 in size are small relative to its expectation.

Interday dynamics. At the beginning of day $i > 0$, one samples N new founder individuals out of the γN cells from the population at the end of day $i - 1$. We assume that one of these new founders carries a *beneficial* mutation with probability μ_N ; otherwise (with probability $1 - \mu_N$), there is no beneficial mutation. We think of μ_N as the probability that in the course of day $i - 1$ a beneficial mutation has occurred, one of whose offspring is sampled for day i . Strictly speaking, μ_N should be considered as the expected number of new

beneficial mutants in the sample of size N at the next morning. As long as μ_N is not very small, precision may be added by using Poisson random variables, which is what we do in the simulations, see Appendix. One might also think of an even finer ‘intraday modelling’ of the mutation mechanism, cf. Wahl and Zhu (2015) or LeClair and Wahl (2018). However, because of the design of the LTEE ($N \approx 5 \cdot 10^6$, $\gamma \approx 100$), it does not seem likely that this should lead to substantial clustering phenomena (or even heavy tails) in the distribution of the number of new beneficial mutants in the next morning.

Assume now that, when a mutation occurs, it affects a uniformly chosen individual among the N founders at the beginning of day i ; say this is individual number m . Its reproduction rate is then increased via

$$r_{im} \rightarrow r_{im} + \delta(r_{im}) \quad \text{with } \delta(r) := \frac{\varphi_N}{r^q}. \quad (7)$$

Here, φ_N scales the beneficial effect and q determines the strength of epistasis. In particular, $q = 0$ implies constant increments (that is, additive fitness), whereas $q > 0$ means that the increment decreases with r , that is, we have diminishing returns epistasis. Note that, at this stage, the fitness increment is deterministic (given the current r_{im}), in line with the *staircase model* of population genetics (Fisher 1918; Desai and Fisher 2007). In contrast, the fitness effects follow an exponential distribution in Wisner et al. (2013); we will turn to stochastic increments in Sec 3.2. Note also that we have idealised by not taking into account the change in fitness due to mutation during the day; this seems to be a valid approximation since a mutation occurring during the day will not rise to appreciable frequency in the course of this first day of its existence, and thus will not change the overall growth rate of the population in any meaningful way.

Scaling regime. We have indexed μ_N and φ_N with population size because the law of large numbers requires to consider a sequence of processes indexed with N and to take the limit $N \rightarrow \infty$. More precisely, we will take a *weak mutation — moderate selection limit*, which requires that μ_N and φ_N become small as N goes to infinity in some controlled way. Specifically, we assume

$$\mu_N \sim \frac{1}{N^a}, \quad \varphi_N \sim \frac{1}{N^b} \quad \text{as } N \rightarrow \infty, \quad 0 < b < \frac{1}{2}, \quad a > 3b. \quad (8)$$

This entails that φ_N is of order greater than $1/\sqrt{N}$ but less than 1, and μ_N is of much lower order than φ_N . Note that μ_N is the mutation *probability per population*, and (8) assures that μ_N and the fitness advantage it conveys are both very small, so that it is highly unlikely that there is more than one new mutant at every given day; this is why we neglect this possibility for the purpose of the analysis. Furthermore, the scaling of φ_N implies that selection is stronger than genetic drift as soon as the mutant has reached an appreciable frequency.

Relative fitness process. The obvious notion of mean relative fitness is the expectation of the empirical relative fitness in (1), that is,

$$\mathbb{E}\left(\frac{\log(Y_i(T_i)/Y_i(0))}{\log(Y_0(T_i)/Y_0(0))}\right). \quad (9)$$

For the sake of mathematical tractability, however, we instead define the mean relative fitness at day i as

$$F_i^N := \frac{\log(\mathbb{E}(Y_i(T_i))/Y_i(0))}{\log(\mathbb{E}(Y_0(T_i))/Y_0(0))}. \quad (10)$$

This is a valid approximation to (9) for a reason similar to that given below (6): For large $Y_i(0)$, the fluctuations of $Y_i(T_i)/Y_i(0)$ are small relative to their expectation, so the moment closure underlying the use of (10) instead of (9) seems justified. Assuming that $Y_i(0) = N$ and setting $t_i = R_0 T_i$, where T_i is again the time until the nutrients are used up, (10) turns into

$$F_i^N = \frac{1}{t_i} \log\left(\frac{1}{N} \sum_{j=1}^N e^{r_{ij} t_i}\right) \quad (11)$$

since $r_{0j} \equiv 1$, so $\mathbb{E}(Y_0(T_i))/Y_0(0) = e^{t_i}$. Note that (11) implies that

$$e^{F_i^N t_i} = \frac{1}{N} \sum_{j=1}^N e^{r_{ij} t_i}, \quad (12)$$

which means that F_i^N may be understood as the *effective reproduction rate* of the population at day i , which is different from the mean Malthusian fitness $\frac{1}{N} \sum_j r_{ij}$ unless the population is homogeneous, that is, $r_{ij} \equiv r_i$.

Let us now consider the *relative fitness process* $(F_i^N)_{i \geq 0}$. Qualitatively, the Cannings model displays the same behaviour as in the classical models of population genetics, such as the Wright-Fisher or Moran model, in the case of weak mutation and moderately strong selection; see, e.g., Graur and Li (2000, Ch. 2 and Fig. 2.7). Two distinct scenarios can happen: either a fast loss of a new beneficial mutation, or its fixation. Furthermore, with the chosen scaling, the population turns out to be homogeneous for almost all i as $N \rightarrow \infty$, which has the following bunch of practical consequences.

First, on a time scale with a unit of $1/(\mu_N \varphi_N)$ days, $(F_i^N)_{i \geq 0}$ turns into a jump process as $N \rightarrow \infty$, cf. Fig. 3. Second, F_i^N in (11) does not depend on the chosen duration t_i (or T_i , respectively), which is why these quantities need not be specified more precisely. Third, in (11), we assume size N for each of the competing samples, whereas this size is only $N/2$ in the real-life competition experiment; but again this yields the same F_i^N in a homogeneous day- i population. And fourth, $F_i^N = \frac{1}{N} \sum_j r_{ij}$ in a homogeneous population, so the effective reproduction rate coincides with the mean Malthusian fitness.

Heuristics leading to the limit law. Assume a new mutation arrives in a *homogeneous* population of relative fitness F . It conveys to the mutant individual a relative *fitness increment*

$$\delta_N(F) = \frac{\varphi_N}{F^q}, \quad (13)$$

that is, the mutant has (relative) Malthusian fitness $F + \delta_N(F)$. The length of the growth period then is

$$\sigma(F) = \frac{\log \gamma}{F} \quad (14)$$

(since this solves $e^{Ft} = \gamma$, cf. (6)). We now define the *selective advantage* of the mutant as

$$s_N(F) = \delta_N(F) \sigma(F). \quad (15)$$

Let us explain the reasoning behind this identification. In population genetics, the selective advantage (of a mutant over a wildtype) per generation is

$$s = \frac{a_1 - a_0}{a_0}, \quad (16)$$

where a_0 (a_1) is the expected number of descendants of a wildtype (mutant) individual in one generation. If growth is in continuous time with Malthusian parameters r_0 and $r_1 = r_0 + \delta$, respectively, and a generation takes time σ , then $a_0 = e^{r_0\sigma}$ and $a_1 = e^{r_1\sigma} \approx a_0(1 + \delta\sigma)$ if δ is small, which turns (16) into (15). Often, the appropriate notion of a generation is the time until the population has doubled in size, see e.g. formula (3.2) in Chevin (2011), which provides an analogue to (15)). In our setting, the corresponding quantity is the time required for the population to grow to γ times its original size, which is the length $\sigma(F)$ of the growth period in (14).¹ Together with the above expression for s , this explains (15).

Notably, a formula that is perfectly analogous to (15) appears in Sanjuán (2010, p. 1977, last line); there, the concept of a viral generation is associated with the cell infection cycle, and the number K (which corresponds to our γ) is the burst size or viral yield per cell.

It is precisely the notion of selection advantage conveyed by (15) and (16) that governs the *fixation probability*. Namely, the fixation probability of the mutant turns out to be

$$\pi_N(F) \sim C s_N(F). \quad (17)$$

Here, \sim means asymptotic equality (that is, $\pi_N(F)/(C s_N(F)) \rightarrow 1$ as $N \rightarrow \infty$, see González Casanova et al. (2016)), and $C := \gamma/(\gamma - 1)$ is 1/2 times the offspring variance over one day in the underlying Cannings model. Hence (17) is in line with Haldane's formula, which says that the fixation probability is the selective advantage divided by half the variance of the offspring size in one generation. Haldane's formula relies on a branching process approximation

¹In line with this, we choose days as our discrete time units, as already mentioned in Sec 1.

of the initial phase of the mutant growth; see Patwa and Wahl (2008) for an account of this method, including a historic overview.

Obviously, *the length σ of the growth period decreases with increasing F* and, since s_N in (15) decreases with decreasing σ , we would observe a decrease of s_N with increasing F even if $\delta_N(F)$ were constant. This is what we call the *runtime effect*: Adding a constant to an interest rate F of a savings account becomes less efficient if the runtime decreases.

Another crucial ingredient of the heuristics is the time window of length

$$u_N(F) = \frac{\log N}{s_N(F)} \quad (18)$$

after the appearance of a beneficial mutation that will survive drift (a so-called *contending mutation*) in the fitness background F ; this is the expected time it takes for the mutation to become dominant in the population.

All this leads us to the dynamics of the relative fitness process. As illustrated in Fig. 3, most mutants only grow to small frequencies and are then lost again (due to the sampling step). But if it does happen that a mutation survives the initial fluctuations and gains appreciable frequency, then the dynamics turns into an asymptotically deterministic one and takes the mutation to fixation quickly, cf. Durrett (2008, Ch. 6.1.3). Indeed, within time $u_N(F)$, the mutation has either disappeared or gone close to fixation; by (8), this time is much shorter than the mean interarrival time $1/\mu_N$ between successive mutations. As a consequence, there are, with high probability, at most two types present in the population at any given time (namely, the *resident* and the *mutant*), and *clonal interference is absent*. Therefore, in the scenario considered, fixation is equivalent to survival of drift.

Next, we consider the expected per-day increase $\Delta_N F$ in relative fitness, given the current value F . This is

$$\mathbb{E}(\Delta_N F | F) \approx \mu_N \pi_N(F) \delta_N(F) \sim \frac{\Gamma_N}{F^{2q+1}}. \quad (19)$$

Here, the second equality is due to (13)–(17), and the compound parameter

$$\Gamma_N := C \mu_N \varphi_N^2 \log \gamma \quad (20)$$

is the rate of fitness increase per day at day 0 (where $F_0 \equiv r_0 = 1$). Note that φ_N/F^q appears squared in the asymptotic equality in (19) since it enters both π_N and δ_N . Note also that the additional +1 in the exponent of F comes from the factor of $1/F$ in the length of the growth period (14), and thus reflects the runtime effect.

We now define a new time variable τ related to i of (3) via

$$i = \left\lfloor \frac{\tau}{\Gamma_N} \right\rfloor \quad (21)$$

with Γ_N of (20), which means that one unit of time τ corresponds to Γ_N days. With this rescaling, we have

$$F_{\lfloor \tau/\Gamma_N \rfloor}^N \rightarrow f(\tau) \text{ as } N \rightarrow \infty,$$

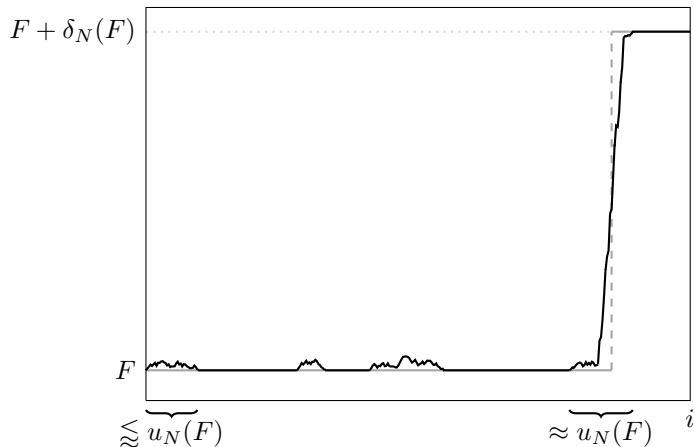


Figure 3: The relative fitness process (black) and the approximating jump process (grey).

where f satisfies the initial value problem

$$\frac{d}{d\tau} f(\tau) = \frac{1}{f^{2q+1}(\tau)}, \quad f(0) = 1, \quad (22)$$

with solution

$$f(\tau) = \left(1 + 2(1+q)\tau\right)^{\frac{1}{2(1+q)}}. \quad (23)$$

Note that (22) is just a rescaling limit of (19), where the expectation was omitted due to the scaling regime applied, as will be explained next.

Law of large numbers. The precise formulation of the limit law (González Casanova et al. 2016) reads

Theorem *Under the scaling (8), the sequence of processes $(F_{\lfloor \tau/\Gamma_N \rfloor}^N)_{\tau \geq 0}$ converges for $N \rightarrow \infty$, in distribution and locally uniformly, to the deterministic function f in (23).*

The theorem was proved along the heuristics outlined above² with the help of advanced tools from probability theory. It is a law of large numbers in the sense that, for large N and under the scaling assumption (8), fitness is the sum of a large number of small per-day increments accumulated over many days, and may be approximated by its expectation. It is this kind of reasoning which allows to go from (19) to (22) (and thus to ‘sweep the expectation under the carpet’).

Since time has been rescaled via (21), Eq. (23) has q as its single parameter. Note that $1/(2(1+q)) < 1$ (leading to a concave f) whenever $q \geq 0$; in particular,

²Note that González Casanova et al. (2016) partly work with dimensioned variables, which is why the notation and the result look somewhat different.

the fitness curve is concave even for $q = 0$, that is, in the absence of epistasis. This is due to the runtime effect: if the population as a whole already reproduces rather fast, then the end of the growth phase is reached sooner and thus leaves less time for a mutant to play out its advantage; see also the discussion in Sec. 4. The second parameter, namely Γ_N , reappears when τ is translated back into days; that is, $F_i^N \approx f(\Gamma_N i)$. Note that R_0 , as used in the first nondimensionalisation step (4), is not an additional parameter because it is already absorbed in φ_N^2 .

A first reality check. The limit law (23) is identical with the power law (2) of Wisner et al. (2013) up to renaming of parameters and change of time scale. We have $q = g - 1$, so $\hat{g} = 5.2$ of Sec. 1 translates into $\hat{q} = 4.2$.³ Furthermore, $\Gamma = \beta \log_2 \gamma / (2(1 + q))$ due to Eqns. (2) and (23) together with the fact that $k = \tau \log_2 \gamma / \Gamma$ by (3) and (21); given $\hat{\beta} = 5.2 \cdot 10^{-3}$, this results in $\hat{\Gamma} = 3.2 \cdot 10^{-3}$ (here and in what follows, we suppress the index N , since we will work with fixed, finite N from now on). The resulting fit is reproduced in Fig. 4 (red solid line). For the purpose of comparison, we average over all 12 populations (with the hypermutator populations included, as in Wisner et al. (2013), Fig. 2), but are aware of a certain variability of the parameters between the populations, see their Table S4.

In the light of (20), of the given value $\hat{\Gamma}$, and of the fact that $C \log \gamma \approx 4.7$, the values of $\hat{\mu}$ and $\hat{\varphi}$ cannot both be very small. We therefore now check the limit law against realistic parameter values.

We start by decomposing the compound parameter Γ . It is useful to denote the *mean fitness increment due to the first fixed beneficial mutation* by

$$\mathfrak{d}_1 := \delta(F_0). \quad (24)$$

This was estimated as $\hat{\mathfrak{d}}_1 = 0.1$ by Lenski et al. (1991), see also Gerrish and Lenski (1998), and Wisner et al. (2013); it implies $\hat{\varphi} = 0.1$ due to (13) and $F_0 = 1$. For reasons to be explained in Sec. 3.1, however, we work with the somewhat larger value $\hat{\mathfrak{d}}_1 = \hat{\varphi} = 0.14$. The mutation probability may then be obtained from (20) as

$$\hat{\mu} = \frac{\hat{\Gamma}}{C \hat{\varphi}^2 \log \gamma} = 0.035 \quad (25)$$

Stochastic simulations of the GKWY model, performed with Algorithm 1 described in the Appendix and using the above parameters together with $N = 5 \cdot 10^6$, are also shown in Fig. 4. Their mean (over 12 simulation runs) recovers the basic shape of the fitness curve, but systematically underestimates both the limit law and the data. A natural explanation for this is clonal interference, which is absent in the limit under the scaling (8), but leads to loss of mutations for finite N . This will be taken into account in the next section. But let us note here that the fluctuations in the data are rather larger than those of the

³Recall that we denote parameter estimates by a hat to distinguish them from the corresponding theoretical quantities. Figures are rounded to two digits.

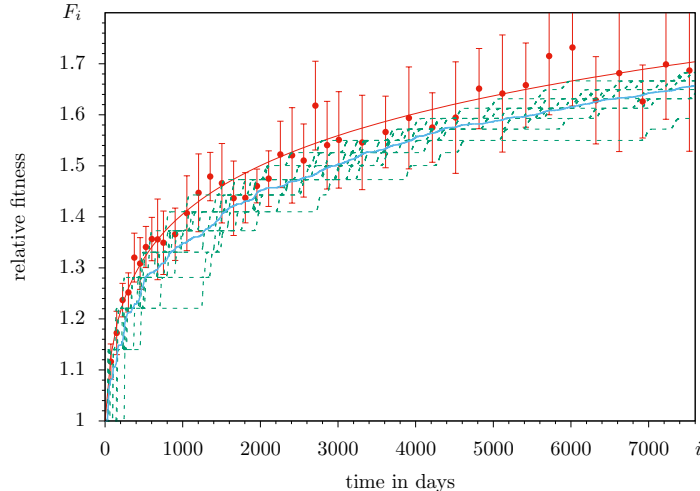


Figure 4: Least-squares fit of law of large numbers (23) to the data in Wisner et al. (2013), and stochastic simulations of finite populations with deterministic beneficial effects. Red bullets: mean empirical relative fitness (averaged over all 12 populations) as in Fig. 2, with error bars (95% confidence limits based on the 12 populations) from Wisner et al. (2013); solid red line: $F_i \approx f(\hat{\Gamma}i)$ with parameter values $\hat{q} = 4.2$ and $\hat{\Gamma} = 3.2 \cdot 10^{-3}$; green lines: 12 individual trajectories F_i obtained via Cannings simulations with $N = 5 \cdot 10^6$, $\gamma = 100$, $\hat{\varphi} = 0.14$, and $\hat{\mu} = 0.035$; light blue line: average over the 12 simulations.

simulations; this may well go along with a variability of the parameters between the 12 replicates of the LTEE, which is present in the data, but not in our simulations.

3 Including clonal interference

As discussed in the previous section, the scaling regime in the GKWY model was such that, with high probability, no new beneficial mutation arrived while the previous one was on its way either to extinction or fixation. As emphasised already in González Casanova et al. (2016), and as indicated by the simulation results in Figure 4, also clonal interference should be taken into account. Briefly stated, clonal interference refers to the situation where a second contending mutation appears while the previous one is still on its way to fixation. It is crucial to keep in mind that, unlike the case without clonal interference considered in Sec. 2, survival of drift may then no longer be identified with fixation; rather, there may be an additional loss of contending mutations due to clonal interference. In particular, the quantity π of (17) must now be addressed as the probability to survive drift.

A full analytic treatment of clonal interference is beyond the scope of this paper; in particular, we will not prove a law of large numbers here. Rather, we adapt the heuristics of Gerrish and Lenski (1998), see also Wisner et al. (2013). The heuristics was originally formulated for fitness effects that follow an exponential distribution. We will, however, first consider the deterministic effects as assumed in the GKWY model in Sec. 3.1 and then proceed to random effects from an arbitrary probability distribution in Sec. 3.2.

3.1 Deterministic beneficial effects

For the case of deterministic beneficial effects, we will sketch and apply a *thinning heuristics*, as a counterpart of the heuristics of Gerrish and Lenski (1998). Consider the situation that a second mutation surviving drift appears within the time window $u(F) := u_N(F)$ of (18) of a first mutation (this is more or less while the first mutation has not become dominant yet). Then, with high probability, the second mutation occurs in an individual of relative fitness F (as opposed to an individual of relative fitness $F + \delta(F)$), and therefore belongs to the same fitness class as the first mutant and its offspring. Thus, as far as fitness is concerned, the two mutants (and their offspring) can be considered equivalent. In our heuristics, the occurrence of a second (and also a third, fourth, . . .) mutation within the given time window neither speeds up nor decelerates the (order of magnitude of) the time until the new fitness class is established in the population. So $u(F)$ plays the role of a *refractory period*, in the sense that the fitness increments carried by contending mutations arriving within this period are lost. The probability that a given increment is *not* lost is determined via the expected waiting time for a (first) contending mutation to appear given the current value F , which is $v_1 := 1/(\mu\pi(F))$, and the expected duration $v_2 := u(F)$ of the refractory period. Specifically, by (17) and (18), the probability in question is

$$\frac{v_1}{v_1 + v_2} \sim \frac{1}{1 + C\mu \log N}. \quad (26)$$

Under this approximation, the expected per-day increase of the relative fitness, given its current value F , turns into

$$\mathbb{E}(\Delta F | F) \approx \frac{\mu \pi(F) \delta(F)}{1 + C\mu \log N} \sim \frac{\Gamma}{F^{2q+1}}, \quad (27)$$

where now

$$\Gamma = \frac{C\mu\varphi^2 \log \gamma}{1 + C\mu \log N}, \quad (28)$$

that is, the factor μ in (20) is replaced by $\mu/(1 + C\mu \log N)$. Now, taking the expectation over F in (27) yields

$$\mathbb{E}(\Delta F) \approx \Gamma \mathbb{E}\left(\frac{1}{F^{2q+1}}\right) \gtrsim \frac{\Gamma}{(\mathbb{E}(F))^{2q+1}}.$$

Here, the second step is due to Jensen’s inequality.⁴ The interchange of the expectation with this function reflects a crude way of moment closure. We therefore arrive at the approximation

$$\mathbb{E}(F_{\lfloor \tau/\Gamma \rfloor}) \approx f(\tau) \text{ for large } N$$

with f as in (23), and may, therefore, again approximate the data by the function f , with the same values $\hat{\varphi}$ and $\hat{\Gamma}$ as before. The compound parameter Γ , however, has an internal structure different from the previous one (compare (28) with (20)). Solving (28) for μ gives

$$\mu = \frac{\Gamma}{C(\varphi^2 \log \gamma - \Gamma \log N)}; \quad (29)$$

for our current $\hat{\Gamma}$ and $\hat{\varphi}$, this yields $\hat{\mu} = 0.079$ and thus a better agreement between the simulated mean fitness and the approximating power law (and hence with the data), see Fig. 5. Notably, $\hat{\mu}$ is of the same order of magnitude as $1/\log N = 0.15$; for an asymptotic analysis as $N \rightarrow \infty$, this would imply that the ratio (26) is bounded away from 0. For substantially higher mutation probabilities, the heuristics would break down and a different asymptotic regime would apply (Durrett and Mayberry 2011).

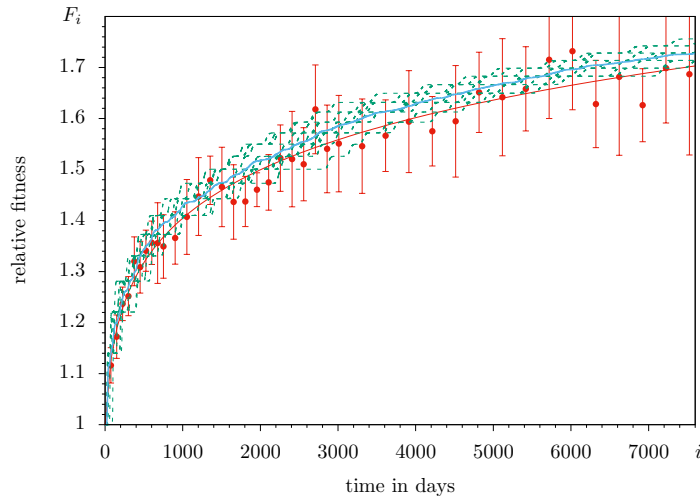


Figure 5: Canning simulation as in Fig. 4, but with mutation probability $\hat{\mu} = 0.079$.

Let us now investigate the remaining discrepancy between the mean of the Canning simulations and the approximating power law. Since the power law has been obtained via two approximations, namely the thinning heuristics and moment closure, it is interesting to quantify the contributions of these two sources

⁴Note that $1/x^p$ is a convex function of x for any $p \geq 1$.

of error. To this end, we simulate the evolution according to the heuristics rather than the Cannings model (see Algorithm 2 in the Appendix). The result is shown in Fig. 6. The simulation mean is very close to that of the Cannings simulation. We may conclude that the heuristics approximates the Cannings model very well, at least at the level of the mean values; the discrepancy between the Cannings simulation and the power law should therefore mainly be ascribed to moment closure. Note that the simulation of the heuristics yields smaller fluctuations than that of the Cannings model; this is in line with expectations, since the heuristics contains fewer random elements than the original model.

Let us finally comment on our choice $\hat{\varphi} = 0.14$. The denominator of (29) is strictly positive, and hence μ is finite (and positive), as long as

$$\varphi > \sqrt{\frac{\hat{\Gamma} \log N}{\log \gamma}} = 0.10.$$

The existence of such a lower bound on φ is plausible since the refractory period poses an upper bound to the rate of fixation events. Here we work with the value of $\hat{\varphi} = 0.14$ in order to stay reasonably far away from an undesirable ‘explosion’ of $\hat{\mu}$. With this choice, the number of fixed beneficial mutations in the simulation in Fig. 6, averaged over the 12 realisations, is 21; this is to be compared with the estimate of 60–110 fixed mutations observed in 50000 generations by Tenaillon et al. (2016), and of 100 fixed mutations observed in 60000 generations by Good et al. (2017), which both include neutral mutations.

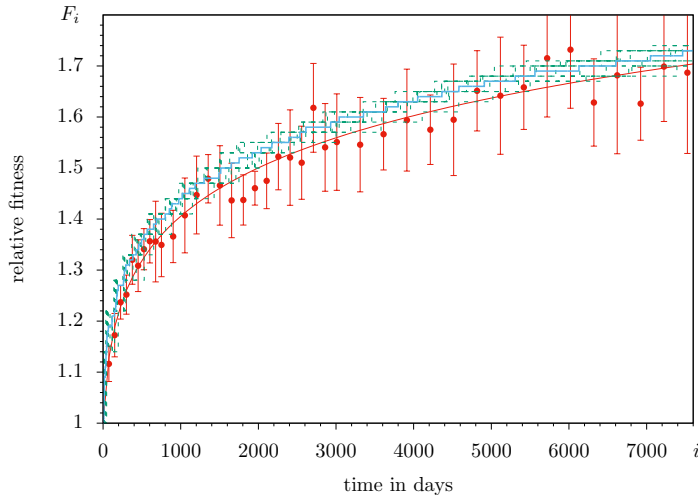


Figure 6: Simulation using heuristics for deterministic increments. Parameters as in Fig. 5. Mean number of clonal interference events: 24; mean number of established mutants: 21.

3.2 Random beneficial effects

Let us now turn to random beneficial effects. To this end, we scale the fitness increments with a positive random variable X with density h and expectation $\mathbb{E}(X) = 1$. We assume throughout that $\mathbb{E}(X^2) < \infty$ to ensure that all quantities required in what follows are well-defined.

Taking into account the dependence on X , the quantities in (13)–(15) and (17)–(18) turn into

$$\delta(F, X) = X \frac{\varphi}{F^q}, \quad (30a)$$

$$\sigma(F) = \frac{\log \gamma}{F} \text{ (as before),} \quad (30b)$$

$$s(F, X) = \delta(F, X) \sigma(F), \quad (30c)$$

$$\pi(F, X) \approx C s(F, X), \quad (30d)$$

$$u(F, X) = \frac{\log N}{s(F, X)}. \quad (30e)$$

Note that large X implies large s and hence small u and vice versa. Note also that (30d) is only an approximation, whereas in (17) we have asymptotic equivalence. The Gerrish-Lenski heuristics for clonal interference, extended to a general distribution of beneficial effects, now reads as follows. If a second contending mutation (with $X' = x'$) appears within time $u(F, x)$ of the first (with $X = x$), then the fitter one wins (that is, the one with $\max\{x, x'\}$). Thus, for given F the probability that a contending mutation with fitness effect x survives clonal interference is approximately

$$\begin{aligned} & \exp\left(-u(F, x) \int_x^\infty \mu \pi(F, x') h(x') dx'\right) \\ & \approx \exp\left(-\mu \frac{C \log N}{x} \int_x^\infty x' h(x') dx'\right) =: \psi(\mu, x). \end{aligned} \quad (31)$$

Notably, ψ does not depend on F . Thus we obtain, as an analogue of (27), the expected (per-day) increase of F , given the current value of F , as

$$\begin{aligned} \mathbb{E}(\Delta F | F) & \approx \mu \int_0^\infty \delta(F, x) \pi(F, x) \psi(\mu, x) h(x) dx \\ & \approx \frac{C \mu \varphi^2 \log \gamma}{F^{2q+1}} \int_0^\infty x^2 \psi(\mu, x) h(x) dx \\ & = \frac{\Gamma}{F^{2q+1}}, \end{aligned} \quad (32)$$

where

$$\Gamma := C \mu \varphi^2 \log \gamma I(\mu) \quad (33)$$

and $I(\mu)$ is the integral in (32). A moment closure argument as in Sec. 3.1 (and, in a suitable parameter regime, presumably also a law of large numbers

reasoning as in Sec. 2) leads to

$$\mathbb{E}(F_{[\tau/\Gamma]}) \approx f(\tau).$$

The parameter Γ can then be estimated from the empirical data in the same way as described at the end of Sec. 2. In order to decompose Γ with the help of the observed mean fitness increment of the first fixed beneficial mutation (in analogy with (25)), we note that the density of X , conditional on fixation and as a function of F , is obtained by reweighting the original density h with the (conditional) probabilities to survive drift and clonal interference, which yields

$$h(x \mid \text{fixation}) = \frac{h(x)\pi(F, x)\psi(\mu, x)}{\int_0^\infty h(x')\pi(F, x')\psi(\mu, x') dx'} \sim h(x) \frac{x\psi(\mu, x)}{\mathbb{E}(X\psi(\mu, X))}.$$

This means that conditioning on fixation introduces a *size bias* into the distribution of beneficial effects, as already observed by Rozen et al. (2001) and Wisner et al. (2013) in the case of the exponential distribution. In line with this, the expected increment conditional on fixation reads

$$\mathbb{E}(\delta(F, X) \mid \text{fixation}) = \frac{\mathbb{E}(\delta(F, X)\pi(F, X)\psi(\mu, X))}{\mathbb{E}(\pi(F, X)\psi(\mu, X))} \approx \frac{\varphi}{F^q} \zeta(\mu) \quad (34)$$

with

$$\zeta(\mu) := \frac{\mathbb{E}(X^2\psi(\mu, X))}{\mathbb{E}(X\psi(\mu, X))}.$$

Note that, under the assumptions on X , $\zeta(\mu)$ is well defined for any μ , since $0 < \psi \leq 1$.

Since the initial value of F is 1, the observable value for the mean fitness increment due to the first fixed beneficial mutation thus suggests to translate (34) into

$$\mathfrak{d}_1 := \mathbb{E}(\varphi X \mid \text{fixation}) \approx \varphi \zeta(\mu). \quad (35)$$

In contrast to the deterministic case (24) (with or without clonal interference), the relationship between \mathfrak{d}_1 and φ is complicated due to the additional nonlinear factor $\zeta(\mu)$. But (33) together with (35) tells us that, given $\widehat{\Gamma}$, the estimated mutation probability $\widehat{\mu}$ is the (numerical) solution of

$$\frac{\widehat{\mu}I(\widehat{\mu})}{(\zeta(\widehat{\mu}))^2} = \frac{\widehat{\Gamma}}{C \log \gamma \widehat{\mathfrak{d}}_1^2}. \quad (36)$$

The analysis so far allows to conclude that, as long as the approximation (via the heuristics and moment closure) may be relied on, the *mean fitness curve* observed by Wisner et al. (2013) *can be described by any distribution of fitness effects*, provided the mutation probability is chosen according to (36) (and provided that (36) has a solution). In particular, the *epistasis parameter* \widehat{q} is *not affected by the choice of the distribution of X* .

Exponentially-distributed beneficial effects. For definiteness, we now turn to exponentially distributed effects, where X follows $\text{Exp}(1)$, the exponential distribution with parameter 1. This is the canonical choice since strongly-beneficial mutations appear to be exponentially distributed, as reviewed by Eyre-Walker and Keightley (2007); the distribution of slightly-beneficial mutations is less well known, but these mutations contribute little to the adaptive process. For such an X , (36) and (35) together give $\hat{\mu} = 0.43$ and hence $\hat{\varphi} = 0.040$ for $\hat{\delta}_1 = 0.14$ (as in Sec. 2 and Sec. 3.1). Fig. 7 shows the corresponding Cannings simulations, and Fig. 8 contains the simulations according to the heuristics. The agreement of the simulation mean with the approximating power law is now nearly perfect. The fluctuations, however, are smaller in the simulations than in the experiment. As argued in Sec. 2 in the context of the first reality check, this may be explained by the constant parameters assumed by the model, whereas parameters do vary across replicate populations in the experiment.

Let us also mention the degree of polymorphism observed in the Cannings simulations of Fig. 7. Counting a type as ‘present’ if its frequency is at least 20%, we observe that, on average, the population is monomorphic on 81% of the days; it contains two types on 18% of the days, and three types on 1% of the days. Thus, in the finite system, some polymorphism is present, but it is not abundant.

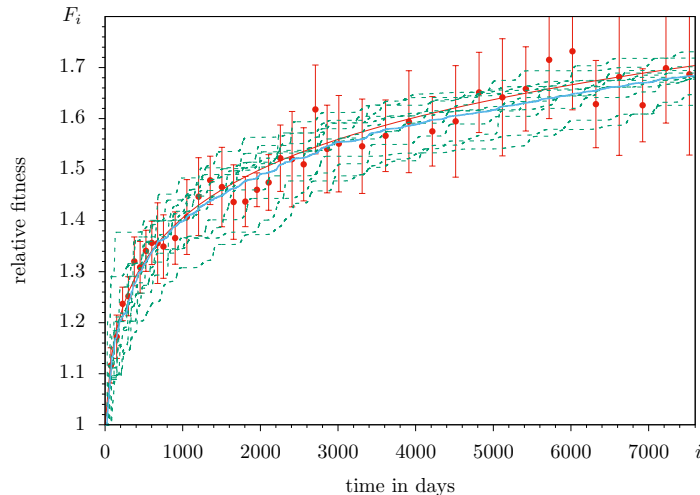


Figure 7: Cannings simulations as in Fig. 5, but with X following $\text{Exp}(1)$, $\hat{\varphi} = 0.04$, and mutation probability $\hat{\mu} = 0.43$.

Beneficial effects with a Pareto distribution. As argued already, the exponential distribution seems to be the most realistic choice for beneficial mutation effects. The theory developed above, however, holds for arbitrary proba-

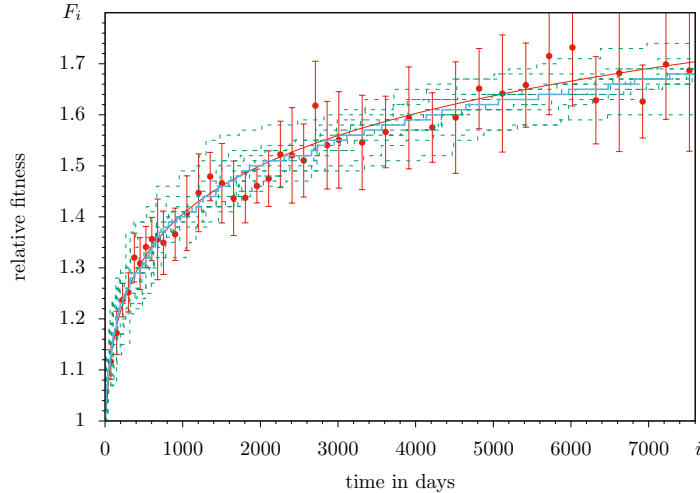


Figure 8: Simulations using Gerrish-Lenski heuristics with X following $\text{Exp}(1)$ and parameters as in Fig. 7. Mean number of clonal interference events with $x' \leq x$: 36; mean number of clonal interference events with $x' > x$: 22; mean number of established beneficial mutants: 39.

bility distributions on the positive half axis that have expectation 1 and a finite second moment. Furthermore, the analysis of the heuristics indicates that the results are, in fact, independent of the distribution, provided the compound parameter Γ is interpreted in the appropriate way. It is therefore interesting to explore whether this conclusion may be verified by simulations. In order to push our conjecture to the limits, we choose X distributed according to a (*shifted*) *Pareto distribution* (see Feller (1971, Ch. II.4) or Stuart and Ord (1994, Ex. 2.19)) with shape parameter a as given by the density

$$h(x) = \begin{cases} 0, & x < 0 \\ \frac{a}{a-1} \left(\frac{a-1}{x+(a-1)} \right)^{a+1}, & x \geq 0. \end{cases} \quad (37)$$

The parameter $a \geq 0$ controls which of the moments of X exist. For $0 < a \leq 1$, the expectation is infinite; for $1 < a < 2$, the expectation is 1 but the second moment is infinite; for $2 < a \leq 3$, $\mathbb{E}(X) = 1$ and $\mathbb{E}(X^2) = 2(a-1)/(a-2)$ but the third moment is infinite; and similarly for larger a . We work with $a = 2.5$ here; this implies that there is no restriction in applying our analysis.

Proceeding in analogy with the case of exponentially distributed beneficial effects, we simulate both the Cannings model and the heuristics and compare them with the approximating power law. For (36) to have a solution, it is required that

$$\hat{\mathfrak{d}}_1 > \frac{\hat{\Gamma}(\zeta(1))^2}{C \log \gamma I(1)} \approx 0.23;$$

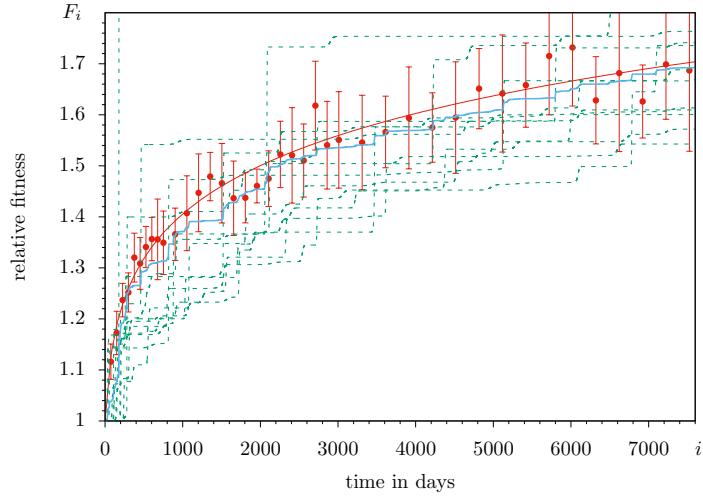


Figure 9: Simulations of the Cannings model with X following the (shifted) Pareto distribution with density h of (37). Parameters: $a = 2.5$, $\hat{\varphi} = 0.030$, and $\hat{\mu} = 0.14$.

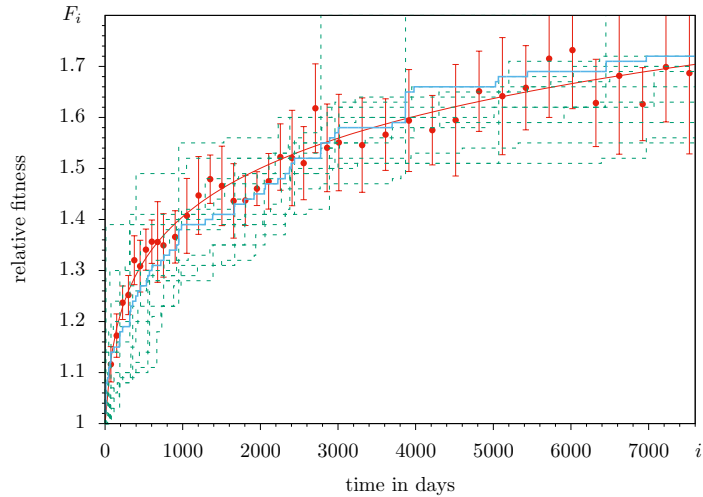


Figure 10: Simulations using Gerrish-Lenski heuristics with X following the (shifted) Pareto distribution and parameters as in Fig. 9. Mean number of clonal interference events with $x' \leq x$: 4.6; mean number of clonal interference events with $x' > x$: 5.4; mean number of established beneficial mutants: 16.

we work with $\hat{\delta}_1 = 0.3$. The result is shown in Figs. 9 and 10. As was to be expected, the mean is still well described by the approximating power law, but

the fluctuations are enhanced relative to the case of the exponential distribution (note that now $\mathbb{E}(X^2) = 6$ in contrast to $\mathbb{E}(X^2) = 2$ in the case of $\text{Exp}(1)$, and thus, by (36) and (35), we have $\hat{\mu} = 0.14$ and hence $\hat{\varphi} = 0.03$). Compared to the experiment, the fluctuations are unrealistically large; an effect distribution with high variance therefore does not appear to be close to the truth.

4 Discussion

We have, so far, postponed a detailed comparison with the model and the results of Wisner et al. (2013). We now have everything at hand to do so.

Modelling aspects. Both the WRL model and ours lead to power laws, (2) and (23), which are identical up to renaming of parameters and change of time scale. But the modelling assumptions differ in relevant details, with consequences for the interpretation of the parameters.

The main difference is that Wisner et al. (2013) use a *Wright-Fisher* model to describe the experiment, and approximate the effect of the variable population size caused by daily sampling and regrowth with the help of an effective population size, which is constant over time. In contrast, we have modelled the daily cycling explicitly with the help of a *Cannings* model, thus obliterating the need to work with an effective population size. This sheds light on the dynamics *within a day* and reveals the *runtime effect*, that is, the shortening of the daily growth period with increasing fitness. Let us emphasise that this runtime effect is a consequence of the design of Lenski's experiment; it would be absent in a variant of the experiment in which sampling occurs at a given fixed time before the onset of the starvation phase.

A consideration of the runtime effect is implicit (though somewhat difficult to detect) in Wisner et al. (2013). Indeed, the WRL model works with *multiplicative* fitness effects (caused by the beneficial mutations), whereas we use *additive* fitness effects. Let us recall that the (intraday, dimensionless) Malthusian growth rate r coincides with the relative fitness F defined in (11), at least for a (nearly) homogeneous population, cf. (12); this is because we used a scaling of time such that r_0 , the growth rate at day zero, equals 1. On the other hand, F is an (individual-based) equivalent of the relative fitness w as defined by Wisner et al. (2013, supplement, p. 3).

Formula (S5) of Wisner et al. (2013) says that the multiplicative effect on r has expected size $1/\alpha$; this corresponds to an additive effect on r of expected size r/α . The assumption (S1) in Wisner et al. (2013) states that the probability π that a beneficial mutation survives drift is (on average) equal to 4α . As can be seen from the discussion after our Eq. (15), the factor r between the fixation probability π and the additive effect on the Malthusian fitness must come from a consideration of the runtime effect. In the light of Haldane's formula, the different factors in the survival probability (the factor of 4 in (S1) of Wisner et al. (2013)) and the factor $C \approx 1$ in our Eq. (17)) must come from different offspring variances. At least qualitatively, this points in the right direction, because

the offspring variance over a day (which is the concept of generations in our Cannings model) is certainly larger than the offspring variance over a “doubling time” (which underlies the generation scheme in the WRL model). It seems, however, that our model, with its closer relation to the design of the LTEE, gives a clearer access to the relevant population size and the appropriate offspring variance in Haldane’s formula.

Another interesting issue is the interpretation of *diminishing returns epistasis*, and the corresponding translation between the exponent g in the WRL model and the exponent q in ours. As a matter of fact, undamped multiplicative effects (which correspond to $g = 0$ in Wisner et al. (2013), see their formula (S6)) lead to an exponential growth of the relative fitness (see their (S8); the fact that this growth is not super-exponential is due to the runtime effect). Note also that the power law approximation (S16) is only defined for $g > 0$. The choice $g = 1$ in the WRL model (or equivalently, $q = 0$ in ours, cf. (2) and (23)) corresponds to *additive* increments on the Malthusian fitness that do not depend on the current value of the latter, see (13). Indeed, (S9) shows that, for $g = 1$, the multiplicative increment $1/\alpha$ is proportional to $1/F$ and hence corresponds to a constant *additive* increment. It is this case of constant additive increments which may be appropriately addressed as the *absence of epistasis*. More precisely, in *continuous time* (as considered here), additive fitness increments correspond to independent action of mutations and hence to absence of epistasis (Fisher (1918); Bürger (2000, pp. 48 and 74)); in *discrete time*, the same is true of multiplicative increments. Consequently, $q = g - 1$ can be seen as an exponent describing the effect of epistasis. Remarkably, the mean fitness curve is (slightly) concave even in the absence of epistasis; this is due to the runtime effect.

A substantial part of the derivations of Wisner et al. (2013) deals with incorporating the Gerrish-Lenski heuristics for *clonal interference* into their model. The fact that they work with multiplicative fitness increments and various approximations complicates the translation between the time-scaling constant β in their power law (see our Eq. (2), which is their formula (S16)) and our time scaling constant Γ (see (23) and (33)). We refrain from pursuing the details here; but let us emphasise that (30) together with the calibrations discussed in Sec. 3.2 applies to arbitrary random (additive) fitness effects with finite second moments.

Analytic and simulation results. We have presented three lines of results. First, rigorous results for the relative mean fitness in terms of a law of large numbers in the limit $N \rightarrow \infty$ for deterministic beneficial effects in a regime of weak mutation and moderately strong selection. Second, we have derived transparent analytic expressions for the *expected* mean fitness in a finite- N system by means of heuristics of Gerrish-Lenski type and a moment closure approximation (which is also used by Wisner et al. (2013)). The beneficial effects may be either deterministic (and then require a specific thinning heuristics), or random with an arbitrary density (here the original Gerrish-Lenski heuristics applies). As it

turned out, the analytic expressions are *robust*. In particular, the estimate of q is neither affected by clonal interference nor by the choice of the distribution. What changes is the internal structure of the compound parameter Γ , but for any given estimate $\hat{\Gamma}$, the mutation probability and scaling of beneficial effects may be arranged appropriately (provided X has second moments). The deviations from $q = 0$ are a signal of diminishing returns epistasis; at this point, let us again emphasise that the approximating curve of the mean relative fitness is (slightly) concave even for $q = 0$ (due to the runtime effect). By any means, the pronounced concavity in the curve approximating the LTEE data (with its estimated $\hat{q} = 4.2$) gives strong evidence for diminishing returns epistasis.

Our third line of investigations is a simulation study both of the Cannings model and the approximating heuristics. Here it turned out that the heuristics approximates the Cannings model very well (it might be improved even further by taking into account the refined heuristics of Gerrish (2001) and Rozen et al. (2001)). This suggests that the discrepancy between the (mean of the) Cannings simulations and the approximating power law is mainly due to moment closure. The simulations show that this deviation is moderate for deterministic increments, minute for exponential increments, and hard to quantify for Pareto increments due to the large fluctuations.

Appendix: Simulation algorithms

Let us briefly describe the two algorithms we have used to simulate our model. Before we come to the details, let us say a few words about notation and strategy. We will throughout use the framework (30), which reduces to (13)–(15) and (17)–(18) in the case of deterministic beneficial effects, where $X \equiv 1$, that is, the distribution of X is a point measure on 1. (But note that, in Sec. 3.2, we assume that X has a density; this implies that any two realisations of X are different with probability 1, so that there is a clear ‘winner’ in the Gerrish-Lenski heuristics. The analysis of Sec. 3.2 therefore does not carry over to the deterministic case.) *Curly* symbols indicate *sets* of values, whereas *bold* symbols indicate *lists* and $\bullet^{(k)}$ their k -th element. By slight abuse of notation, we denote by δ (δ^\uparrow) the increment of relative fitness (30a) for the current (previous) mutation.

Algorithm 1 performs an individual-based simulation of the Cannings model with selection, as formulated in Section 2. Its iterations are based on real-world days i . The algorithm keeps track of the sizes \mathcal{N}_j of the classes (or subpopulations) of individuals that have reproduction rate \mathcal{R}_j , $j \geq 1$. As long as n_{typ} , the number of different reproduction rates in the population, equals 1, the population is homogeneous, so that the intraday growth and subsequent sampling do not change the current state. If $n_{\text{typ}} > 1$, we use the fact that the clone size at time σ in a Yule process with branching rate \mathcal{R}_j started by a single individual is 1 plus a random variable that follows $\text{Geo}(e^{-\mathcal{R}_j\sigma})$, the

geometric distribution⁵ with parameter $e^{-\mathcal{R}_j\sigma}$ (cf. Feller (1968, Ch. XVII.3) or Durrett (2008, Ch. 1.3.3)). The size of the corresponding subpopulation at time σ is then \mathcal{N}_j plus the sum of \mathcal{N}_j independent copies of the geometric random variable. This sum follows $\text{NB}(\mathcal{N}_j, e^{-\mathcal{R}_j\sigma})$, the negative binomial distribution with parameters \mathcal{N}_j and $e^{-\mathcal{R}_j\sigma}$, cf. Feller (1968, Ch. VI.8) or Stuart and Ord (1994, pp. 168/169). The only point where each individual must be treated separately is the sampling step, where $N = 5 \cdot 10^6$ new founder individuals are drawn without replacement from the $\approx 5 \cdot 10^8$ descendants. After the sampling, the number of mutation events is drawn from $\text{Poi}(\hat{\mu})$, the Poisson distribution with parameter $\hat{\mu}$ (line 13). The affected individuals are then chosen *uniformly without replacement* from among the N new founders.

Algorithm 2 unifies the two versions of the thinning heuristics of Sec. 3. We now only keep track of substitutions that effectively lead to an increase of the relative fitness, and thus have a homogeneous population in every iteration k . The number k counts the fixation events, and the vector ι holds the times at which they occur. More precisely, mutations appear after waiting times Δ_ι following $\text{Exp}(\hat{\mu})$ (approximating the discrete $\text{Geo}(\hat{\mu})$ -distribution). For every such mutation, it is decided whether or not it survives drift by drawing a Bernoulli random variable with success probability π according to (30d) (line 13). If the mutation survives, it is queried whether it survives clonal interference. We simulate this by first adding the increment δ^\uparrow due to a ‘first’ mutation to the mean fitness, and then adding the additional increment $\delta - \delta^\uparrow$ due to the ‘second’ mutation if it outcompetes the former. For the choice $X \equiv 1$, this means that the first out of two competing mutations wins; the case of **A fitter mutation appeared** in line 7 can never occur for deterministic increments.

For the sake of completeness, the parameter combinations for the simulations in this paper are summarised in Tab. 1.

Law of X	ι_{\max}	\hat{q}	$(\hat{\mathfrak{d}}_1)$	$\hat{\mu}$	$\hat{\varphi}$	Algo. 1	Algo. 2
$\equiv 1$	7600	4.2	(0.14)	0.035	0.14	Fig. 4	
$\equiv 1$	7600	4.2	(0.14)	0.079	0.14	Fig. 5	Fig. 6
$\text{Exp}(1)$	7600	4.2	(0.14)	0.43	0.04	Fig. 7	Fig. 8
shifted Pareto, $a = 2.5$, cf. (37)	7600	4.2	(0.3)	0.14	0.03	Fig. 9	Fig. 10

Table 1: Summary of parameter values for simulations. The population size and the dilution factor have been fixed as $N = 5 \cdot 10^6$ and $\gamma = 100$ throughout.

⁵We take $\text{Geo}(p)$ as the distribution of the numbers of failures before the first success in a coin tossing with success probability p .

Algorithm 1: Simulating Lenski's experiment (Cannings model)

Input: User chosen density law of X and parameters $\iota_{\max}, \hat{q}, \hat{\mu}, \hat{\varphi}$.

- 1 **Initialise** $k = 0, \sigma = 1, n_{\text{typ}} = 1, n_{\text{mut}} = 0, \mathcal{R} = \{1\}, \mathcal{N} = \{N\}$.
- 2 **while** $k < \iota_{\max}$ **do**
 - // Length of intraday growth time
 - 3 Solve (6), i.e. $\sum_{j=1}^{n_{\text{typ}}} \mathcal{N}_j e^{\mathcal{R}_j \sigma} = \gamma N$, to obtain σ .
 - 4 Set $\mathbf{F}^{(k)}$ according to (11).
 - 5 **if** $n_{\text{typ}} > 1$ **then**
 - // Intraday population growth
 - 6 $n_{\text{des}} \leftarrow 0$.
 - 7 **for** $j = 1, \dots, n_{\text{typ}}$ **do**
 - 8 \lfloor Draw $D \sim \text{NB}(\mathcal{N}_j, e^{-\mathcal{R}_j \sigma})$ and set $n_{\text{des}} \leftarrow n_{\text{des}} + \mathcal{N}_j + D$.
 - // Interday sampling
 - 9 Draw sample $\{j_1, \dots, j_N\}$ without replacement from $\{1, \dots, n_{\text{des}}\}$ and set $\mathcal{N} = \{\mathcal{N}_1, \dots, \mathcal{N}_{n_{\text{typ}}}\}$ accordingly.
 - 10 **for** $j = 1, \dots, n_{\text{typ}}$ **do**
 - 11 **if** $\mathcal{N}_j = 0$ **then**
 - 12 \lfloor Remove type j and set $n_{\text{typ}} \leftarrow n_{\text{typ}} - 1$.
 - // Mutation
 - 13 Draw $n_{\text{mut}} \sim \text{Poi}(\hat{\mu})$ and set $n_{\text{typ}} \leftarrow n_{\text{typ}} + n_{\text{mut}}$.
 - 14 **if** $n_{\text{mut}} > 0$ **then**
 - 15 Draw sample $\{i_1, \dots, i_{n_{\text{mut}}}\}$ without replacement from $\{1, \dots, N\}$.
 - 16 **for** $j = 1, \dots, n_{\text{mut}}$ **do**
 - 17 $\mathcal{N}_{i_j} \leftarrow \mathcal{N}_{i_j} - 1$ and $\mathcal{N} \leftarrow \mathcal{N} \cup \{1\}$.
 - 18 Draw X and set $\mathcal{R} \leftarrow \mathcal{R} \cup \{\mathcal{R}_{i_j} + \delta(\mathcal{R}_{i_j}, X)\}$ acc. to (30a).
 - 19 **if** $\mathcal{N}_{i_j} = 0$ **then**
 - 20 \lfloor Remove type i_j and set $n_{\text{typ}} \leftarrow n_{\text{typ}} - 1$.
- 21 $k \leftarrow k + 1$.
- 22 **return** \mathbf{F} .

Algorithm 2: Simulating Lenski’s experiment (thinning heuristics)

Input: User chosen law of X and parameters $\iota_{\max}, \hat{q}, \hat{\mu}, \hat{\varphi}$.

```
1 Initialise  $k = 0, \iota = 0, \delta = \delta^\uparrow = 0, \iota^{(0)} = 0, \mathbf{F}^{(0)} = 1$ .
2 while not terminated, i.e.  $\iota^{(k)} + \iota \leq \iota_{\max} \wedge k \leq k_{\max}$  do
    // Not within refractory period according to (30e), (30c), (30b)
3   if  $\iota > \log(N)/(\delta^\uparrow \sigma(\mathbf{F}^{(k)}))$  then
    // Beneficial mutant becomes fixed unrivalled
4      $(\iota^{(k+1)}, \mathbf{F}^{(k+1)}) \leftarrow (\iota^{(k)} + \iota, \mathbf{F}^{(k)} + \delta)$ .
5      $(\iota, k, \delta^\uparrow) \leftarrow (0, k + 1, \delta)$ .
6   else
    // A fitter mutation appeared
7     if  $\delta > \delta^\uparrow$  then
8        $(\iota^{(k+1)}, \mathbf{F}^{(k+1)}) \leftarrow (\iota^{(k)} + \iota, \mathbf{F}^{(k)} + \delta - \delta^\uparrow)$ .
9        $(\iota, k, \delta^\uparrow) \leftarrow (0, k + 1, \delta)$ .
    // Occurrence of a next mutant to become dominant
10  do
11    Draw  $X$  and set  $\delta \leftarrow \hat{\varphi}X(\mathbf{F}^{(k)})^{-\hat{q}}$  according to (30a).
12    Draw  $\Delta_\iota$  following  $\text{Exp}(\hat{\mu})$  and set  $\iota \leftarrow \iota + \Delta_\iota$ .
13  while  $S$  following  $\text{Ber}(C\delta\sigma(\mathbf{F}^{(k)}))$  is unsuccessful according to (30d)
14 return  $(\iota, \mathbf{F})$ .
```

Acknowledgements

It is our pleasure to thank Phil Gerrish for valuable hints and comments on the manuscript. We also thank Richard Lenski for stimulating discussions. This project received financial support from Deutsche Forschungsgemeinschaft (German Research Foundation, DFG) via Priority Programme SPP 1590 *Probabilistic Structures in Evolution*, grants no. BA 2469/5-1 and WA 967/4-1.

References

- J.E. Barrick, D. S. Yu, S. H. Yoon, H. Jeong, T. K. Oh, D. Schneider, R. E. Lenski, and J. F. Kim, Genome evolution and adaptation in a long-term experiment with *Escherichia coli*, *Nature* **461** (2009), 1243–1247.
- R. Bürger, *The Mathematical Theory of Selection, Recombination, and Mutation*, Wiley, Chichester, 2000.
- L.M. Chevin, On measuring selection in experimental evolution, *Biology Letters* **7** (2011), 210–213.
- M.M. Desai and D. S. Fisher DS, Beneficial mutation-selection balance and the effect of linkage on positive selection, *Genetics* **176** (2007), 1759–1798.

- R. Durrett, *Probability Models for DNA Sequence Evolution*, 2nd ed., Springer, New York, 2008.
- R. Durrett and J. Mayberry, Travelling waves of selective sweeps, *Ann. Appl. Prob.* **21** (2011), 699–744.
- W.J. Ewens, *Mathematical Population Genetics*, 2nd ed., Springer, New York, 2004.
- A. Eyre-Walker and P.D. Keightley, The distribution of fitness effects of new mutations, *Nature Reviews Genetics* **8** (2007), 610–618.
- W. Feller, *An Introduction to Probability Theory and its Applications*, Vol. I, 3rd ed., Wiley, New York, 1968.
- W. Feller, *An Introduction to Probability Theory and its Applications*, Vol. II, 2nd ed., Wiley, New York, 1971.
- R. Fisher, The correlation between relatives on the supposition of Mendelian inheritance, *Phil. Trans. R. Soc. Edinburgh* **52** (1918), 399–433.
- P.J. Gerrish and R.E. Lenski, The fate of competing beneficial mutations in an asexual population, *Genetica* **102/103** (1998), 127–144.
- P.J. Gerrish, The rhythm of microbial adaptations, *Nature* **413** (2001), 299–302.
- A. González Casanova, N. Kurt, A. Wakolbinger, and L. Yuan, An individual-based model for the Lenski experiment, and the deceleration of the relative fitness, *Stoch. Proc. Appl.* **126** (2016), 2211–2252.
- B.H. Good, M.J. McDonald, J.E. Barrick, R.E. Lenski, and M.M. Desai, The dynamics of molecular evolution over 60,000 generations, *Nature* **551** (2017), 45–50.
- D. Graur and W.-H. Li, *Fundamentals of Molecular Evolution*, 2nd ed., Sinauer, Sunderland, MA (2000).
- J.S. LeClair and L.M. Wahl, The impact of population bottlenecks on microbial adaptation, *J. Stat. Phys.* (2017), <https://doi.org/10.1007/s10955-017-1924-6>
- R. Lenski, M.R. Rose, S. Simpson, and Tadler, Long term experimental evolution in *Escherichia coli* I. Adaptation and divergence during 2000 generations, *Amer. Nat.* **138** (1991), 1315–1341.
- R. E. Lenski and M. Travisano, Dynamics of adaptation and diversification: a 10,000-generation experiment with bacterial populations, *Proc. Natl. Acad. Sci. U.S.A.* **91** (1994), 6808–6814.
- S.-C. Park, J. Krug, Clonal interference in large populations, *Proc. Natl. Acad. Sci. U.S.A.* **104** (2007), 18135–18140.

- Z. Patwa and L.M. Wahl, The fixation probability of beneficial mutations, *J. R. Soc. Interface* **5** (2008), 1279–1289.
- P. Phillips, S. Otto, and M. Whitlock, Beyond the average: the evolutionary importance of gene interactions and variability of epistatic effects, in “Epistasis and the Evolutionary Process” (J. Wolf, E. Brodie, and M. Wade, Eds.), 2000, pp. 20–38, Oxford University Press, Oxford.
- D.E. Rozen, J.A.G.M. de Visser, and P.J. Gerrish, Fitness effects of fixed beneficial mutations in microbial populations, *Current Biology* **12** (2002), 1040–1045.
- R. Sanjuán, Mutational fitness effects in RNA and single-stranded DNA viruses: common patterns revealed by site-directed mutagenesis studies, *Phil. Trans. R. Soc. B* **365** (2010), 1975–1982.
- A. Stuart and K.J. Ord, *Kendalls Advanced Theory of Statistics (Vol. 1, Distribution Theory)*, 5th ed., Wiley, Chichester 1994.
- O. Tenaillon, J. E. Barrick, N. Ribeck, D. E. Deatherage, J. L. Blanchard, A. Dasgupta, G. C. Wu, S. Wielgoss, S. Cruveiller, C. Medigue, D. Schneider, and R. E. Lenski, Tempo and mode of genome evolution in a 50,000-generation experiment, *Nature* **536** (2016), 165–170.
- L. Wahl and A.D. Zhu, Survival probability of beneficial mutations in bacterial batch culture. *Genetics* **200** (2015), 309–320.
- M.J. Wisner, N. Ribeck, and R.E. Lenski, Long-term dynamics of adaptation in asexual populations, *Science* **342** (2013), 1364–1367
- M.J. Wisner, N. Ribeck, and R.E. Lenski, Data from: Long-term dynamics of adaptation in asexual populations, Dryad Digital Repository.